Neuron, Vol. 15, 299–310, August, 1995, Copyright © 1995 by Cell Press

Systematic Widespread Clonal Organization in Cerebral Cortex

Christopher B. Reid,*†‡ Ivan Liang,* and Christopher Walsh*†
*Department of Neurology
†Program in Neuroscience
Program in Biological and Biomedical Sciences
Beth Israel Hospital
Harvard Medical School
Boston, Massachusetts 02115
‡Washington University School of Medicine
St. Louis, Missouri 63110

Summary

Cell lineage analysis in the cortex has revealed two clonal patterns, clustered and widespread clones. To determine the relationship of these patterns, progenitor cells were infected with a retroviral library encoding alkaline phosphatase, and cortical sibling cells were identified using PCR. Clones labeled at E15 consisted of single cells or small cell clusters (52%) or of widespread cells (48%). However, widespread clones consisted of multiple neuronal or glial cell types, spaced systematically at 2–3 mm intervals. The data suggest that migratory multipotential progenitors divide asymmetrically at intervals defined by cell cycle length, producing single cells or clusters of cells in different cortical regions. Transition from multipotentiality to more restricted potential may correspond to changes in migratory behavior.

Introduction

The mammalian cerebral cortex is composed of diverse and highly differentiated neuronal and glial cell types. The cortex is parceled into functionally specialized regions with distinct cellular architectures, but across cortical regions, there is conservation of intrinsic and extrinsic circuitry and cellular morphologies (Beaulieu and Colonnier, 1989). Cortical neurons arise from progenitor cells that line the lateral ventricle in the ventricular and subventricular zones. The manner, however, in which germinal zone progenitors divide to produce multiple cortical cell types remains largely unclear.

Transplantation studies have suggested that some aspects of cortical neuronal identity, such as laminar fate, become fixed during the mitotic phase of the progenitor's cell cycle (McConnell and Kaznowski, 1991). Likewise, other transplantion experiments addressing the neuronal expression of region-specific molecular markers have suggested that there is a plastic period very early in cortical neurogenesis in which progenitor cells remain responsive to environmental signals prior to generating postmitotic daughter cells (Barbe and Levitt, 1991; Ferri and Levitt, 1995). In contrast, progenitor cells from a slightly more mature cortex appear to be less responsive to their host environment (Barbe and Levitt, 1991; Cohen-Tannoudji et al., 1995). The mechanisms of these commitment steps remain unclear, largely because transplantation experiments have advanced ahead of fundamental information about normal progenitor cell behavior.

Experiments tracing cortical cell lineage have relied heavily on replication-defective retroviral vectors that encode histochemical marker genes; these vectors mark daughter cells in clonal fashion. To date, retroviral lineage experiments have provided evidence for progenitors that produce similar neuronal types, defined morphologically or neurochemically (Parnavelas et al., 1991; Grove et al., 1993; Luskin et al., 1993; Mione et al., 1994), or uniform glial types (Luskin et al., 1988, 1993; Goldman and Vaysse, 1991; Grove et al., 1993) over multiple cell divisions. In addition, in vitro (Temple, 1989; Reynolds and Weiss, 1992; Davis and Temple, 1994) and retroviral (Price and Thurlow, 1988; Walsh and Cepko, 1988, 1992) data suggest that a small but significant proportion of cortical progenitors are multipotential and produce diverse cell types. Multipotential progenitors have been observed in other regions of the developing vertebrate nervous system (Holt et al., 1988; Turner et al., 1990; Gray and Sanes, 1991).

The interpretation of retroviral lineage studies in the cerebral cortex is hampered by the fact that cortical sibling cells can migrate in many directions (Walsh and Cepko, 1988). A more recent approach to lineage analysis utilizes libraries of retroviral vectors carrying distinguishable DNA tags that indicate clonal relationships directly. Previous results with the retroviral library technique indicated that the progeny of some cortical progenitors disperse over large distances, in some cases approaching the entire length of the cerebral cortex (Walsh and Cepko, 1992, 1993). One mechanism producing widespread clonal dispersion in the cortex appears to be the migration of progenitor cells within the proliferative zones at rates of 5–20 μm/hr, averaging ~100 μm over 8 hr (Fishell et al., 1993). A second mechanism of clonal dispersion may be the substantial nonradial migration of a minority (~12%) of postmitotic neurons (O'Rourke et al., 1992).

The widespread dispersion of neuronal clones and the surprising migratory behavior of progenitor cells raise the question of how the widespread dispersion of many cortical clones can be reconciled with the apparent clustering of retrovirally labeled cells with similar phenotype. A new retroviral library that encodes alkaline phosphatase (AP) as a histochemical marker provides intense staining of cellular processes and direct determination of cell identity (Fields-Berry et al., 1992). Data obtained using this new retroviral library suggest that widespread clones consist of multiple, distinct clusters of cells, with each cluster "subunit" essentially indistinguishable from the clusters described previously. The presence, however, of multiple subunit clusters within widespread clones suggests a hierarchical model of cortical neuron formation.

Results

Neuronal Progenitors Infected by AP-Encoding Retroviruses Appear to Show Normal Behavior

Cortical progenitors were infected by injection of the AP-encoding retroviral library into the lateral ventricles of fetal rats at embryonic day 14 (E14), E15, or E17. When injected animals were analyzed at postnatal day 15 (P15), retrovirally encoded AP was seen to produce intense labeling of cellular processes, allowing morphological identification of >90% of labeled cells as neuronal or glial by standard morphological criteria. Neurons usually occurred as single cells or small clusters (≤6 cells) and were identifiable by their large (>10 μm diameter) cell somata and by the presence of radiating dendrites often outfitted with spines (Figure 1). Astrocytes occurred as densely packed clusters of tiny cells with overlapping processes that were often so intensely stained in the AP reaction that precise determination of glial type and cell number was sometimes impossible. Since most oligodendrocytes are formed after P15, they were labeled relatively infrequently.

Unlike retrovirally encoded β-galactosidase (Grove et al., 1993), retrovirally encoded AP frequently produced a Golgi-like filling of neuronal processes, including in some cases axons. The morphologies of retrovirally labeled neurons were similar to those seen in postmortem stains of fixed tissue (Werner et al., 1985) (Figures 1a–1d), suggesting that retrovirally encoded AP did not change the morphology of labeled cortical neurons. Pyramidal neurons could be identified by their pyramidal cell bodies, prominent apical and basal dendrites (Feldman, 1984), and frequent spines (Figure 1b). Several types of nonpyramidal cells were seen (Fairen et al., 1984). Bipolar cells showed single dendrites emerging from each end of the cell body, forming a vertically oriented, narrow dendritic field (Fairen et al., 1984). Bitufted neurons had vertically oriented arrays of axonal branches and broader dendritic fields. Multipolar neurons showed large, multipolar dendritic fields (Figure 1c). Chandelier cells showed multipolar dendritic fields and distinctive axonal plexuses in which the axons ended in vertical strings of boutons. Neuroglioform cells showed small, multipolar dendritic fields with short, smooth, finely beaded dendrites and axonal arborizations that appeared to terminate locally (Fairen et al., 1984). While an unambiguous classification of all cortical neuronal types cannot be made on the basis of morphological criteria alone (Peters and Jones, 1984), we found that AP staining allowed identification of morphological subtype in ~80% of labeled neurons.

A more stringent assay of the behavior of retrovirally labeled progenitors came from quantitative analysis of labeled neurons in each cortical layer. Since retroviruses

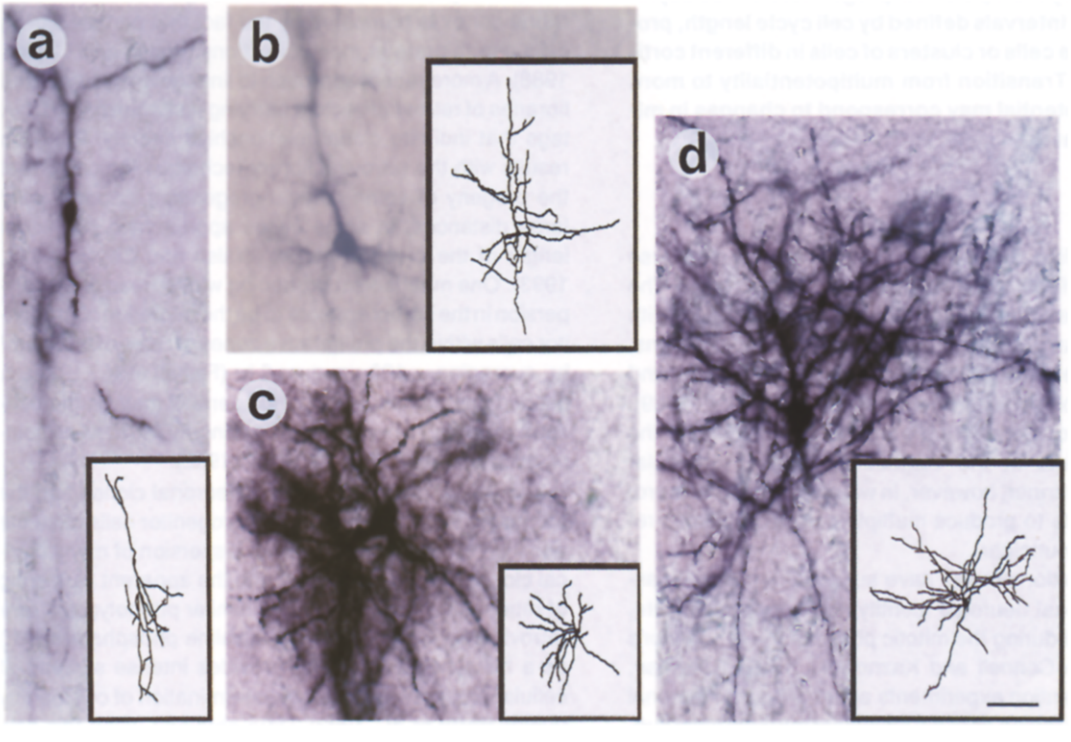

Figure 1. Retrovirally Encoded AP Stains Normal Neuronal Morphology

The photographs show 4 neurons after retroviral injections at E14–E17, with corresponding camera lucida drawings of Golgi-labeled neurons with very similar morphology (Werner et al., 1985). Many different neuronal morphologies can be seen, including a bipolar cell (a), pyramidal cell (b), multipolar cell (c), and basket cell (d). Note that the AP reaction product appears to fill most dendritic processes, as well as the initial axon segment in some cases. The dense filling of neuronal processes allows the additional observation that AP-labeled cells show morphologies indistinguishable from that of unlabeled cells, demonstrating that the AP reaction product does not detectably alter neuronal development. Drawings are used with permission (Werner et al., 1985). Bar, 100 μm.

integrate into the host genome, they label both the older and newer progeny of infected mitotic cells. The "inside-out" generation of the cerebral cortex was reflected in the changing patterns of labeling after retroviral injections at different ages. Injections at E17 labeled a larger proportion of newer neurons (layer II), whereas neurons in deeper layers, known to be largely postmitotic by E17 (Bayer and Altman, 1991), were rarely labeled. In contrast, early injections (E14) labeled neurons in cortical layers IV, V, and VI in much larger proportions (Figure 2). Following E14 injections, 86% of identifiable neurons were pyramidal (25 of 29), consistent with estimates that 70%–90% of neurons in the rat cortex are pyramidal cells (Peters and Kara, 1985; Werner et al., 1985). Later injections labeled progressively fewer pyramidal neurons: 57% after E15 injection (47 of 83) and 42% after E17 injection (25 of 59), with corresponding increases in labeled nonpyramidal neurons. Since pyramidal and nonpyramidal neurons in each cortical layer show overlapping periods of neurogenesis (Miller, 1986), these percentages probably reflect the preferential location of nonpyramidal neurons in the more superficial cortical layers formed relatively later in gestation. We concluded from histological analysis that retroviral labeling did not obviously alter normal cortical neurogenesis or differentiation, that retroviral labeling was not limited to particular neuronal types, and that retrovirally labeled progenitors behaved in a fashion indistinguishable from that of unlabeled progenitors.

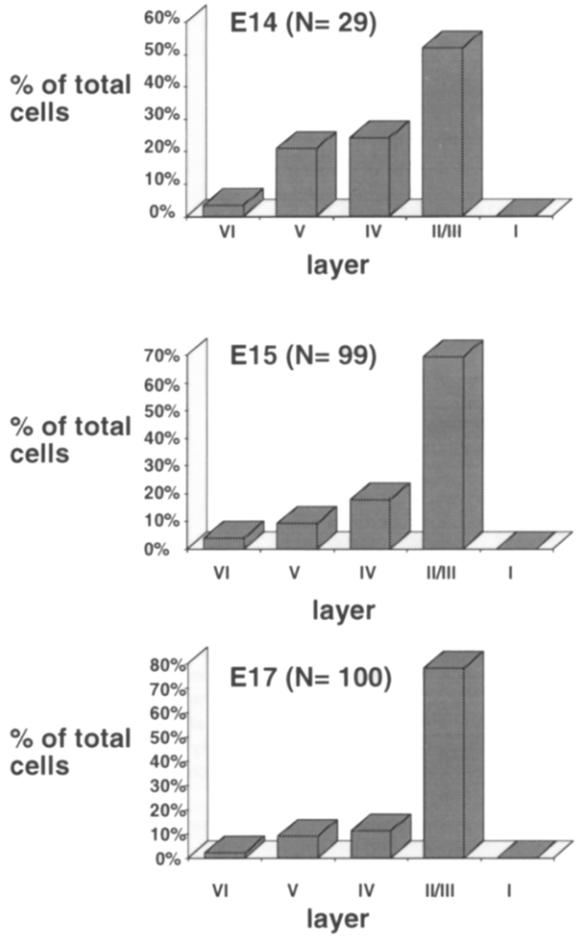

Figure 2. Histograms of Labeled Neurons in Each Cortical Layer of P15 Rat Brains Resulting from Injections at E14, E15, and E17

Retroviruses label the older and newer progeny of infected cells. Neurons in the deepest layers of the cortex are produced first and are largely already generated by the time of the earliest injections. The deep layers are therefore labeled proportionately less than the more superficial layers. The deeper cortical layers also contain fewer neurons than the upper layers (Beaulieu and Colonnier, 1989), exaggerating this effect. Progressively later injections labeled an increasingly restricted population of superficial layer neurons. Laminar patterns of retrovirally labeled neurons are consistent with the timing of neurogenesis determined in birth dating experiments using [^{3}H]thymidine, suggesting that the behavior of infected cortical progenitors is not obviously different from the behavior of unlabeled cortical progenitors.

Clonal Analysis with PCR

Clonal analysis was performed by PCR amplification of retrovirally encoded DNA tags. Cells that contained the same DNA tag were interpreted as originating from the same progenitor cell, while cells with different DNA tags were interpreted as originating from distinct progenitors. The reliability of clonal assignment with retroviral libraries depends upon the degree to which the number of distinct retroviral tags exceeds the number of infective events in each experiment, as coincidental infection of two different progenitors by retroviruses with the same tag produces the spurious appearance of a single clone (Walsh et al., 1992).

The AP-encoding retroviral library was prepared from ~3400 plasmid colonies (Walsh, 1995). The final complexity of the AP-encoding retroviral library was assessed empirically by amplifying DNA tags from clones of NIH 3T3 cells infected in vitro and determining the frequency at which apparently identical tags appeared more than once. The rate of repetition was then used in a Monte Carlo simulation described in detail elsewhere (Walsh et al., 1992) to calculate the complexity of the library and the probability of coincidental double infections by a single tag in any given experiment. In the first in vitro experiment, amplification of 34 clones yielded 2 tags present as duplicates. In a second experiment, amplification of 46 clones yielded 3 duplicate tags and 1 triplicate. The tag present in triplicate in the second experiment matched 1 of the duplicates in the first experiment, and the insert (~190 bp) corresponded approximately in size to the best-known repeated sequence in the Arabidopsis thaliana genome (from which DNA tags were derived; Simoens et al., 1988). The 190 bp tag may be somewhat overrepresented in the library, although it did not appear with high frequency in the in vivo experiments. With the possible exception of the 190 bp insert, the observed repeat rate suggested that ~250–400 other tags, distinguished by restriction enzyme digestion, were present in roughly equal ratios.

Based on the observed repeat rate of tags in the in vitro experiments and on the predicted complexity of the library, Monte Carlo simulations suggested that experiments with <5 clones showed a $p < .05$ probability of containing coincidental double infections, even when the highly repeated

Table 1. Cell Type and Rostrocaudal Position of Clones Labeled by Retroviral Injections at E15

Clone Number	Clusters			
Experiment 1				
1	IV cells (2) [7700]			
2	II/III pyramid [9300]			
3	Cortical astrocytes			
Experiment 2				
4	III neuron [7600][a]	II pyramid [5500]	II np: chandelier [3500]	
Experiment 3				
5	III neuron [11100][b]	II np: multipolar [11000][b]	II/III np: multipolar [8200]	
6	V pyramid [3600]			
7	III pyramid [5900][a]			
8	II pyramid [10800]	IV np: multipolar(2) [58-6200][a]		
9	III pyramid [3800][a]			
Experiment 4[c]				
10	VZ, III pyramids (4) [50-5200][a]			
Experiment 5[c]				
11	Hippocampal pyramid [6700][b]	V pyramid [5100][b]		
12	II pyramid [7000]			
Experiment 6[c]				
13	V pyramid [5000]	IV np [2500][a]		
Experiment 7				
14	VI neuron [10500]	Astrocytes (>3) [8400]	III pyramid (2) [59-6600]	III neuron [3800]
15	II np: bipolar [11500]	III pyramid [8000][b]	II neuron [7700][b]	
16	II np: bipolar [5000]			
17	Piriform neuron [5650]	II cell [2600]		
Experiment 8				
18	IV neuron [4400]			
19	II, IV np: bipolar (2) [49-5200][b]	II/III neuron [4600][b]	II pyramid [2400]	
20	Hippocampal pyramid [10700][b]	II neurons (2) [9800][b]	Hippocampal pyramid [8000][b]	
21	Astrocytes (>3) [6850-7150]			
22	IV inverted pyramid [6950]			
23	Cortical glia (>3) [12100]			
24	II np: multipolar [11100]	II/III pyramid (2) [82-8300]		
25	II/III np: multipolar [12200]	Piriform neuron [5650]		
26	V/VI pyramid [3700]			
27	II neurons (4) [10400]	II np: multipolar (2) [73-8500]	Piriform neuron [5650]	

Clones are from eight experiments, but only five brains, since separate hemispheres of the same brain were considered separate experiments. Widespread clones (48% of total) are divided into columns that represent clusters, defined as ⩾1 sibling cell(s) ⩽1.5 mm from one another and >1.5 mm away from other sibling cells. For each cell or cluster, the distance caudal (in micrometers) to the rostral tip of the olfactory bulb is listed (brackets). Most subunits were separated primarily in the rostrocaudal direction, but some clones had subunits separated ⩾3 mm mediolaterally, at a similar rostrocaudal location. Morphology of cells was determined by AP staining alone, allowing definition of neuronal versus glial identity in > 90% of labeled cells, and allowing identificaiton of broad neuronal classes in ~80% of labeled neurons. Some brains were analyzed at P3; the brain is smaller at this age, and distances between cells/clusters appeared to be correspondingly smaller. Also, not all migration of neurons is complete from the VZ/SVZ at this age. Clone 11 also contained a labeled cell in the striatum/internal capsule, probably a glial cell.

[a] Additional retrovirally labeled, morphologically similar cells were near to the cell indicated but were PCR negative; such cells represent likely sibling cells, but their clonal identity is not certain.

[b] Separated by ⩾3 mm mediolaterally.

[c] Brains analyzed at P3.

tag was analyzed. The viral inoculum was titrated in order to infect <5 clones in most experiments. To bias our data against a major result observed in the study, we analyzed one E17-injected brain that contained 30 clones; this experiment is discussed in detail below. Even in experiments with >5 clones per brain, appearances of the 190 bp tag did not occur in widespread clones, and no discernible difference in clonal patterns was observed between brains with <5 or >5 clones per brain (Table 1; Table 2).

PCR amplification was successful for ~45% of retrovirally labeled tissue samples. Quantitative analysis (data not shown) indicated that AP-positive/PCR-positive neurons showed cell types and laminar distribution indistinguishable from the distribution of all AP-positive cells, suggesting that successful PCR amplification was not preferential for any particular cell type. Efficiency of the PCR reaction was somewhat higher (average ~65%) when β-galactosidase was used as a histochemical marker in similar experiments, suggesting that the AP reaction product may inhibit PCR somewhat. Since the yield of the PCR was less than 100%, the number of sibling cells per clone, and the distribution of sibling cells, is un-

Table 2. Cell Types and Rostrocaudal Position of Clones Labeled by Injections at E17

Clone Number	Clusters	
Experiment 1		
1	Deep entorhinal neuron [13600][a]	IV pyramid [5000]
2	IV neuron [7000]	
3	II neuron [10800]	
Experiment 2		
4	III pyramid [18100]	II np: bipolar [8000]
Experiment 3		
5	Cortical astrocytes (>3)	
6	Cortical astrocytes (>3)	
Experiment 4		
7	III pyramid [12500]	III np:bipolar [3100]
8	II np: bipolar [3200]	
9	Cortical astrocytes (>4)	
Experiment 5		
10	III np: bipolar [8700]	
11	III np: multipolar [9400]	
12	Cortical astrocytes (>3)	
Experiment 6		
13	Perirhinal neuron [14500]	V/VI neuron [8700]
14	II np: bipolar [14400]	Perirhinal neuron [12200]
15	Cortical astrocytes (>8)	
16	Cortical astrocytes (>6)	
17	Cortical astrocytes (>20)	
18	Cortical glia (>1)	
19	Cortical glia (>2)	
20	Cortical glia (>1)	
21	Cortical astrocytes (>3)	
22	Cortical glia (>1)	
23	IV np: neuroglioform [3800]	
24	III np: bitufted [12800]	
25	II/III np: bitufted [15800]	
26	III pyramid [16300]	
27	II np: multipolar [12000]	
28	II np: multipolar [5900]	
29	III np: multipolar [9200]	
30	II np [11200]	
31	III np [18000]	
32	III inverted pyramid [15600]	
33	II cell [12000]	
34	III np: multipolar [5900]	
35	III neuron [6200]	
36	II/III neuron [11900]	
37	Deep perirhinal neuron [17800]	
38	III pyramid [11100]	
39	III pyramid [10600]	
40	II np: multipolar [7600]	

Each experiment represents one hemisphere of five brains analyzed at P15. Other conventions are as in Table 1. Widespread clones were unusual following E17 injection. Unlike widespread clones seen after E15 labeling, widespread clones labeled at E17 contained only 2 cells, each in one of two widely separated locations.

[a] Additonal retrovirally labeled, morpholigically similar cells were nearby (see note to Table 1).

derestimated. No correction was made for this undersampling however, since any numerical corrections would require making assumptions.

Neuronal Clones Formed Two Categories

Clonal analysis of brains injected at E15 or E17 showed two virtually nonoverlapping patterns of clones: widespread clones (defined as clones distributed over >1.5 mm) and clones that consisted of single cells or single clusters of cells grouped within 1 mm (Table 1; Table 2). Of the clones labeled by E15 injections, 52% were clustered or single cells. Clustered clones contained from 3 to >20 glia, or 2–4 morphologically similar neurons within one, or occasionally two, cortical laminae. Clustered clones containing >1 neuron were observed more commonly in retroviral material stained with β-galactosidase than in the present AP material, most likely because the PCR was more efficient in earlier studies (Walsh and Cepko, 1992, 1993). Many of the single-neuron clones listed in Table 1 and Table 2 were part of clusters of mor-

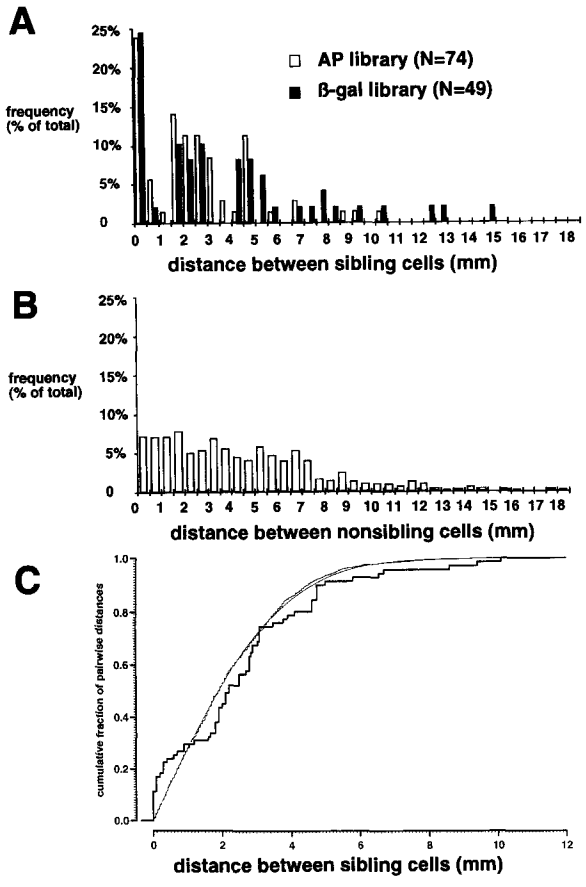

Figure 3. Retrovirally Labeled Sibling Cells Show Nonrandom Spacings

(A) Distances between sibling cells in clones labeled with the AP- or β-galactosidase-encoding retroviral libraries. For AP data (open bars), only rostrocaudal spacing was measured. Measurements were made by counting the number of sections separating cells and multiplying that number by the section thickness (usually 100 μm). For each clone, all possible segments connecting sibling cells were measured. Note that intersibling spacings are very commonly ≤0.5 mm, but rarely 0.5–1.5 mm. Intersibling spacings are also commonly 1.5–3.0 mm, 4–5.5 mm, and possibly 7–8.5 mm, suggesting a reiterated periodic spacing of 2–3 mm between sibling cells. To ensure that the periodicity was not artifactual due to small sample size, previously published data using a β-galactosidase-encoding library (adapted from Walsh et al., 1992) were reanalyzed (closed bars), with distances measured from flat-mounted sections in a direction parallel to the lateral ventricle. Similar preferred spacings were observed in the β-galactosidase material.

(B) Distances between retrovirally labeled nonsibling cells do not show preferred spacings. The histogram shows the distribution of 2239 pairwise rostrocaudal distances (determined as the number of sections between cells multiplied by the section thickness) between retrovirally labeled cells that contained *different* PCR tags. Distances were computed between AP nonsibling cells within the same brain, as well as within littermate brains injected and processed identically (i.e., E15 versus E15 or E17 versus E17). The distribution of pairwise distances appears to approximate a "random" distribution in one dimension (see [C]).

(C) Test of the nonrandom distribution of intersibling intervals. The heavy line shows the cumulative distribution of 71 pairwise rostrocaudal distances among AP-labeled cortical cells with the same tag after E15 labeling. The distribution of intersibling distances differs significantly ($p \approx .003$) from either a model of diffusion by a random walk (smooth curve) or the cumulative distribution of observed pairwise distances between nonsibling cells (B), suitably rescaled (tiny stair steps). The horizontal scale in either model minimizes the largest vertical distance between the observed and model distributions (Kolmogorov–Smirnov distance). The largest differences between the observed and either null hypothesis distribution reflected clustering of sibling cells at <500 μm and the relative absence of intersibling distances of 1.0–1.5 mm. An approximate p value is obtained from simulations (Dallal and Wilkinson, 1986) of Kolmogorov–Smirnov tests against a normal distribution whose mean and SD match the sample moments. The p value is approximate since the present situation differs from that simulated in several respects. One parameter is fit rather than two, and sample moments are not used. The parent distribution is not normal, and the sampling is of cell locations rather than of pairwise distances. Fitting to minimize the Kolmogorov–Smirnov is necessarily conservative, since no other choice of parameter can produce a larger p value. Both the direction and magnitude of the remaining approximations are unknown.

phologically similar cells for which PCR was successful in only 1 cell (see footnotes to Table 1). The finding of clustered neuronal clones confirms earlier descriptions of retrovirally labeled clusters (Parnavelas et al., 1991; Grove et al., 1993; Luskin et al., 1993), which have suggested considerable morphological and biochemical homogeneity among closely clustered retrovirally labeled cells.

Cortical Sibling Cells Were Spaced at Preferred Spatial Intervals

The focus of the present study was the structure of the widespread clones, which are defined by progeny dispersed over >1.5 mm. Widespread clones represented 48% of clones labeled by E15 injections of the AP library (Table 1), a proportion comparable to that seen in recent studies using a β-galactosidase-encoding library (Walsh and Cepko, 1993). A significant majority of retrovirally labeled neurons (73%) were contained in widespread clones. Neurons in widespread clones were spaced preferentially at certain intervals from their siblings. Rostrocaudal distances between sibling cells were determined by counting the number of coronal sections separating sibling cells and multiplying that number by the section thickness (generally 100 μm). Sibling cells were most commonly located 0–0.5 mm from each other. While it was very rare for sibling cells to be spaced 1.0–1.5 mm apart (Figure 3; Table 1; Table 2), it was very common for sibling cells to be spaced 2–3 mm or even 4–6 mm apart, suggesting a periodic spacing of sibling cells corresponding to 2–3 mm in the adult brain. To rule out a spurious periodicity caused by a small sample size, a second previously published data set (Walsh and Cepko, 1992) was reanalyzed in terms of intersibling spacings. This data set showed the same 2–3 mm periodicity (Figure 3).

Periodic spacing of sibling cells within widespread clones could be caused by mechanisms acting within a clone, but could also be caused by nonuniform patterns of neurogenesis or retroviral labeling. These possibilities were distinguished by determining that there was no similar periodicity in the spacing between retrovirally labeled, nonsibling cells within a brain (Figure 3B). Compared with the distribution of nonsibling cells, sibling cells showed a 2.5-fold increased tendency to cluster (i.e., intercell distance of ≤0.5 mm), a 5- to 10-fold *decreased* tendency to

appear 1.0–1.5 mm or 3.5–4 mm apart, and a 1.5- to 2-fold increased tendency to appear 2–3 mm apart. Therefore, a mechanism intrinsic to cortical progenitor cells determines the periodic spacing of their progeny.

To test whether the nonuniform intersibling spacing differed significantly from a random spacing, we compared the intersibling spacings generated by E15 labeling (see Table 1) with a random diffusion model or with the observed spacings between nonsibling cells (Figure 3B). When the test curves were suitably rescaled to minimize the difference from the experimental data by minimizing the Kolmogorov–Smirnov distance (Dallal and Wilkinson, 1986), the intersibling distances still differed significantly ($p \approx .003$) from either test curve (Figure 3C). The greatest difference between the intersibling spacings and the nonsibling spacings occurred at 0–0.50 mm, due to clustering, and at 1.5 mm, a distance at which sibling cells were rarely spaced. We concluded that, while some progenitors produced clustered progeny within 0.5 mm of one another, other progenitors did not form simple clusters, but instead tended to migrate some minimum distance before dividing to form another daughter cell.

Phenotypic Analysis of Clustered and Widespread Clones

Clustered sibling cells showed similar laminar location and morphology (see Table 1; Table 2). Clustered sibling cells (those within 1.5 mm of one another) occurred either in the same layer, or in layers II and III, II and IV, or III and IV. Interestingly, similar patterns were seen regardless of whether the clustered sibling cells were part of a larger, widespread clone or whether they comprised a complete clustered clone (Figure 4; Figure 5). The morphology (Parnavelas et al., 1991; Grove et al., 1993; Luskin et al., 1993), immunohistochemical properties (Mione et al., 1994), and ultrastructure (Parnavelas et al., 1991) of retrovirally labeled neurons that form clusters ≤0.5 mm across have been studied in detail by other labs. The present analysis with AP histochemistry confirms earlier suggestions that clustered clones contain mainly cells of similar morphology.

While clustered sibling cells showed similar location and morphology, widely dispersed sibling cells often showed different phenotypes. Neuronal phenotype can be defined by many cellular features. Most strikingly, some widespread clones contained neurons in both neocortex and piriform/entorhinal cortex (6 of 67 clones; 6 of 18 widespread clones), neocortex and hippocampus (2 of 18 widespread clones), or striatum (1 clone, though the single striatal cell in this clone was probably glial); and the cells in these distinct forebrain structures took on locally appropriate, though widely divergent, morphologies (see Table 1; Table 2). In addition, unlike clustered clones, in which neurons labeled at E15–E17 did not cross layer IV, some widespread clones contained cells in widely different cortical laminae (see Table 1). Furthermore, 2 of 18 widespread clones included neurons in one region and glia in another (see Figure 4), confirming an observation of occasional neuron–glia clones also observed with a β-galactosidase-encoding retroviral library (Walsh and Cepko, 1992, 1993).

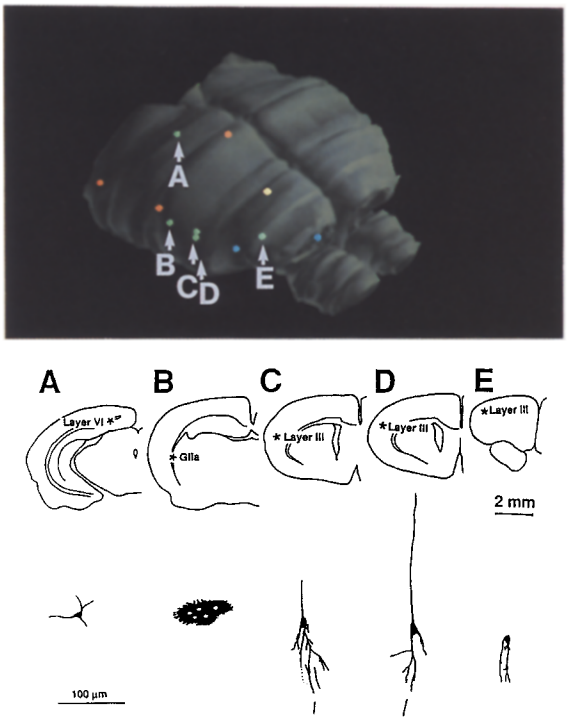

Figure 4. Three-Dimensional Reconstructions of Clones from Experiment 7 That Were Labeled Following Retroviral Injection at E15

Cells that constitute the green clone are illustrated in (A)–(E). (A) represents a layer VI neuron, while 2.1 mm further rostrally, the same clone contains a cluster of several darkly staining astrocytes in the white matter (B). Further rostrally (1.8 mm and 2.5 mm), the same clone contains 2 very similar neurons (layer III pyramidal cells) that are <1 mm from each other (C and D). Finally, 2.8 mm further rostrally, the same clone contains another layer III neuron that is incompletely filled (E).

Finally, 8 of 18 widespread clones contained neurons with nonpyramidal morphology in one neocortical location and pyramidal morphology in another (see Table 1; Figure 5). Neuronal subtype identifications were based on morphological criteria only, rather than combining morphology, ultrastructure, and immunohistochemistry. For example, some multipolar cells in layer IV constitute "star pyramids" that may be functionally related to pyramidal neurons (Peters and Jones, 1984). Nonetheless, of 18 widespread clones (13 from E15, 5 from E17), 17 (94%) contained cells with multiple phenotypes defined either as being located in neocortex plus nonneocortical areas, as being pyramidal plus nonpyramidal neurons, or as being neurons plus glial cells. If widespread clones containing layer IV multipolar neurons were not counted, 14 of 18 widespread clones (78%) still contained cells with multiple phenotypes.

Clones Labeled at E15 Differed Systematically from Those Labeled at E17

When retroviral labeling was performed at E17 rather than E15, the structure of cortical clones was systematically different. Widespread clones were almost 4-fold less common as a percentage of the total number of clones (12.5% versus 48%), a difference significant at $p < .0013$ (χ^2 test). The lower frequency of widespread clones after E17 injec-

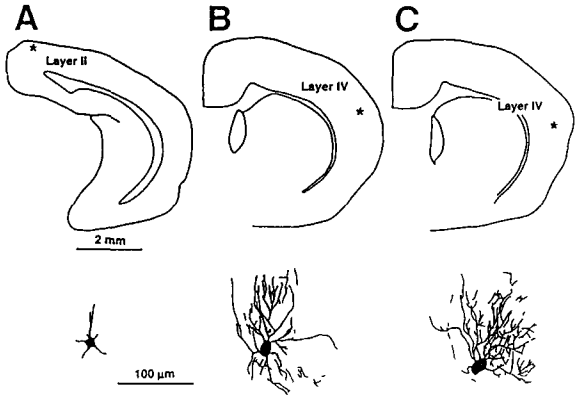

Figure 5. Cell Types in a Widespread Clone from Experiment 3 That Resulted from Retroviral Injection at E15

Specific sections from the coronal series and cells that constitute the widespread clone are drawn in (A)–(C). (B) and (C) are <1 mm apart and show very similar laminar location and morphology (layer IV nonpyramidal, multipolar cells), whereas (A), which is ~4.8 mm away, shows very different morphology (layer II pyramidal neuron). The layer IV neurons did not show obvious spines on their dendrites, suggesting that they are probably not "star pyramids" (Peters and Jones, 1984). Also note that the composition of the 2 subunits of this widespread clone are comparable to other clones that represent single clusters (e.g., clones 1 and 2; see Table 1).

tions was confirmed by performing one E17 experiment with an especially large viral inoculum. If the widespread clones seen after E15 injection were spurious, then widespread clones would be especially common after injection of a large inoculum. However, even injection of a large viral inoculum into a single E17 brain showed a very low incidence (7%) of widespread clones, a pattern very different from that seen after E15 injections (48%).

Widespread clones were not only unusual after E17 injection, they also contained few neurons. All 5 of the widespread clones labeled with the AP-encoding library contained only 2 cells each (Table 3). All widespread clones labeled at E17 with a previous β-galactosidase-encoding library also contained 2 cells each (Walsh and Cepko, 1992). Widespread clones labeled at E17 also accounted for a much lower percentage of the total number of retrovirally labeled neurons (29% versus 73%), suggesting that retroviral injections later in development label progenitors at later stages of neurogenesis.

Discussion

This report characterizes a new retroviral library encoding AP as a histochemical marker and demonstrates that AP-labeled cortical progenitors show proliferative behavior indistinguishable from that of normal progenitors. PCR amplification facilitated determination of clonal relationships among labeled cells. While PCR analysis was not successful for 100% of retrovirally labeled cortical cells, neither was it selective for any particular cell type, and so appeared to provide a fair sample of normal cortical progenitor behavior. Although the clonal patterns represent an end result of many complex developmental processes, including neurogenesis, migration, and cell death, the data suggest some tentative conclusions and a testable model of cortical cell lineage.

Clusters and Widespread Clones

Cortical clones labeled at E15 or E17 were distributed in the cortex as clustered and widespread clones, definable both by location and by cell morphology. Although cells in clustered clones were usually not nearest neighbors (being separated by 300–600 μm typically, i.e., ⩾10 cell diameters), clustered clones imply a progenitor that does not migrate widely as it divides 1–4 times to produce a cluster of a relatively uniform cell type. Clustered clones also show substantial immunohistochemical and ultrastructural uniformity (Parnavelas et al., 1991; Grove et al., 1993; Luskin et al., 1993), suggesting that some progenitors undergo multiple rounds of cell division, producing the same or similar cell types each time.

In contrast, widespread clones consisted of nonrandomly distributed clonal subunits, each subunit being otherwise indistinguishable from a clustered clone. A subunit is defined as 1 or more sibling cells located within 1 mm of one another, and separated from other sibling cells by >1.5 mm. The widespread dispersion of subunits is most easily explained by the migration of progenitor cells. This

Table 3. Comparison of Clonal Patterns after E15 or E17 Injection

	E15	E17
Widespread clones (as percentage of total)	48%	12%
Percentage of neurons that are in widespread clones	73%	29%
Mean number of subunits per widespread clone	2.62	2.0
Maximum number of subunits per widespread clone	4	2
Mean number of neurons per widespread clone	3.23	2.0
Maximum number of neurons per widespread clone	7	2
Mean number of neurons per subunit	1.3	1.0
Maximum number of neurons per subunit	4	1
Mean number of neurons per clustered clone	1.1	1.0
Maximum number of neurons per clustered clone	4	1

Demonstrably widespread clones were observed much more commonly following injections at E15 (48%) than at E17 (12%), a difference significant at $p < .0013$ (χ^2 test). Widespread clones formed after E17 injection contained fewer neurons (maximum of 2) and fewer subunits (only 2 have ever been seen). Clusters and subunits formed after E17 injection also appeared to be somewhat smaller than those formed after E15 injections, although the sample size is small.

migration has been suggested by prior retroviral studies as well as direct in vitro observation (Fishell et al., 1993; Walsh and Cepko, 1993). The periodic spacing of subunits would then be determined by the rate and trajectory of progenitor cell migration and by the length of the progenitor's cell cycle. The distance through which a progenitor moves need not be large to generate the 2–3 mm periodicity seen in the adult brain. The brain increases in length about 4-fold from E18 to P15, so that the 2–3 mm periodicity at P15 corresponds to ~0.5 mm in the E18 cortex, or perhaps 100–250 μm per cell cycle (20–24 hr) in the E18 ventricular zone (Waechter and Jaensch, 1972). This rate of movement is well within the range observed by Fishell et al. (1993). Although most of the movement they observed fit a random walk, migrating cells appeared to be directed systematically rostrally or caudally upon encountering the longitudinal border between cortex and striatum (see their Figure 4), consistent with the pattern of dispersion also suggested by retroviral library analysis after 6 day survival (Walsh and Cepko, 1993). Some AP clones showed strong evidence for systematic spacings of 2–3 mm (see also Figure 6 of Walsh and Cepko, 1992), while others did not, consistent with both systematic and random elements governing the migratory processes that produce widespread dispersion.

A Hierarchical Model of Cortical Plate Lineage

The data suggest a model of cerebral cortical cell lineage (Figure 6) that postulates two types of cortical progenitor cells, distinguishable by their migratory properties and by the fate of their daughter cells. A migratory, multipotential progenitor divides asymmetrically in a stem cell fashion, producing a nonmigratory cell and regenerating a multipotential cell. Nonmigratory cells produced by divisions of the multipotential cell can themselves differentiate or divide 1–4 times to generate multiple cells. Some of the nonmigratory cortical progenitors appear to generate single neuronal types over multiple cell divisions. Labeling of the multipotential progenitor at E15 would provide an equal probability of retroviral integration into the nonmigratory or migratory daughter cell. Integration into the nonmigratory daughter would label a single cluster or single cell, whereas integration into the migratory daughter would label a widespread clone. This might account for the consistent labeling of ~50% clustered and 50% widespread clones in this report and a previous one (Walsh and Cepko, 1993). Each subunit would correspond to a cell cycle of the migratory progenitor, with the observed maximum number of subunits (4) close to the estimated number of remaining neurogenetic cell cycles between E16 and E20 (Waechter and Jaensch, 1972). Retroviral injections at E17 would infect a more mature progenitor with fewer remaining cell divisions. Regardless of which of the 2 daughter cells were labeled by the retrovirus, widespread clones would be labeled less commonly, and the widespread clones would contain fewer subunits, as was observed.

The timing and pace of cortical neurogenesis make it unlikely that alternative models of cell lineage could explain all of our data. Neurogenesis in the cortex proceeds

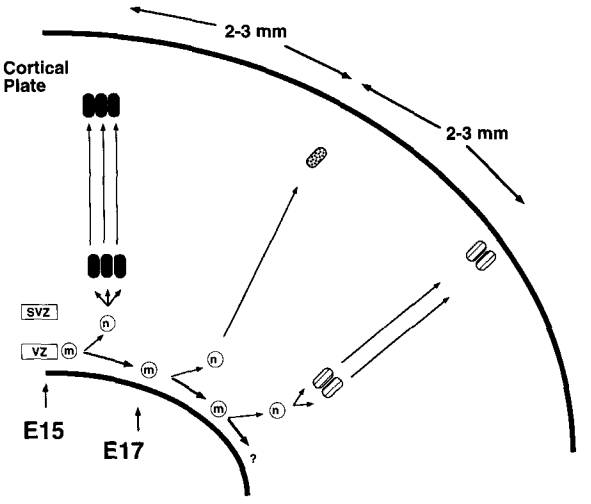

Figure 6. Hypothetical Model of Cell Lineage in the Mammalian Cerebral Cortical Plate

Cerebral cortical cells are derived from two proliferative zones (the ventricular [VZ] and subventricular [SVZ] zones) and migrate from the proliferative zones to the cortex proper. The lineage of 1 multipotential cell is illustrated. The multipotential cell (m) migrates as it divides, sequentially producing 3 nonmigratory progenitors at spatiotemporal intervals and regenerating a multipotential cell in "stem cell" fashion. Each nonmigratory progenitor then behaves essentially independently, dividing more than once (closed cells), directly differentiating (stippled cell), or dividing once (hatched cells), to form 3 distinct cell clusters. Since cells in the rodent cortex are added in a roughly inside-out sequence, the oldest nonmigratory progenitors would tend to form deeper neurons, and the newer nonmigratory progenitors tend to form more superficial neurons. Infection of the multipotential precursor at E15 would result in an equal probability of integration of virus into the migratory or nonmigratory progenitors. Integration into the nonmigratory daughter would label a single clustered clone (or single cell), whereas integration into the migratory daughter would label a widespread clone consisting of several subunits. In contrast, infection at E17 would label a progenitor with fewer remaining cell divisions. No matter which daughter cell the retrovirus integrated into, widespread clones would be rare and small.

from E12 to E20, with the cell cycle length beginning at ~12 hr at E12 and gradually lengthening to 22 hr on E20 (Waechter and Jaensch, 1972; Bayer and Altman, 1991), at which time neurogenesis ceases and gliogenesis continues. A limited number of cell cycles (5–6) is available after E15 infection. Any model that derives all neurons directly from an asymmetrically dividing stem cell could not explain the largest neuronal clones observed (7 neurons) and would not provide a straightforward explanation for the occurrence in a single clone of 2 or more subunit clusters, each composed of multiple cells (see Table 1, clones 14, 20, and 27). A hierarchical model would allow formation of cells "in parallel," allowing generation of larger neuronal numbers over a limited time period.

The proposed model of cortical lineage would reconcile previously conflicting retroviral analyses of cell lineage. Clusters of retrovirally labeled cells with uniform phenotypes (Grove et al., 1993; Luskin et al., 1993; Parnavelas et al., 1991) can be recognized as terminal branches of widespread lineage trees. A transition from a multipotential to a potentially more restricted progenitor also fits well

with previous transplantation studies that suggest that early cortical progenitors are multipotential, but become committed to produce progeny with specific neuronal fates (McConnell and Kaznowski, 1991; Barbe and Levitt, 1991) before completion of the final cell division. The suggestion that migratory progenitors account for the bulk of nonradial clonal dispersion in the cortex would also reconcile the presence of widespread clonal dispersion with the guidance of most postmitotic cortical neurons along radial glial fibers (Rakic, 1972; O'Rourke et al., 1992).

Stem Cell and Non-Stem Cell Progenitors

The existence of multipotential cortical progenitors with stem cell properties has been suggested by recent in vitro studies (Reynolds and Weiss, 1992; Davis and Temple, 1994). Whether the migratory multipotential progenitor described here meets all criteria for a stem cell is uncertain. These criteria include multipotentiality, self-regeneration, and persistence throughout life (Stemple and Anderson, 1992). Persistent cells with stem cell properties have been isolated from the adult brain in the subventricular zone between the striatum and olfactory bulb (Reynolds and Weiss, 1992; Davis and Temple, 1994). A minority (<5%) of retrovirally labeled clones (e.g., P3-M [right] clone C and P3-S [left] clone A in Table 1 of Walsh and Cepko, 1993) also give rise to large numbers of progeny, including multiple cells in the proliferative layers, and may reflect retroviral labeling of true stem cells.

The model of cerebral cortical lineage differs from patterns of cell lineage described in other brain regions and may not apply to all stages of cortical neurogenesis. Progenitors in the retina and tectum do not appear to be highly migratory, and lineage subunits have not been reported in these tissues (Turner et al., 1990; Gray and Sanes, 1991). Very early stages of cortical neurogenesis also may show a remarkable lack of sibling cell dispersion (O'Leary and Borngasser, 1992, Soc. Neurosci., abstract). Perhaps preplate neurons, which appear to form a developmental scaffold for the cortex, follow different rules (Allendoerfer and Shatz, 1994).

The proposed model of cortical development has an important precedent in the CNS of Drosophila melanogaster, where multipotential stem cells termed neuroblasts give rise to ganglion mother cells, which divide once to form pairs of neurons (Campos-Ortega, 1993; Goodman and Doe, 1993). Whereas genetic studies in Drosophila have defined mutations that affect specific steps in invertebrate neurogenesis, the proposed model of cortical cell lineage presents a framework for interpreting defects in vertebrate neurogenesis. For example, genetic disorders that act on migratory versus nonmigratory progenitors should produce very different cerebral cortical phenotypes. The cerebral cortical malformations seen in one disorder, tuberous sclerosis, are thought to be clonal (Gomez, 1988). Tuberous sclerosis shows prominent lesions (cortical tubers) that contain clustered cells with highly differentiated but abnormal morphologies. These lesions may reflect a disorder of the nonmigratory progenitors. Other disorders, such as periventricular heterotopia (Huttenlocher et al., 1994), show abnormal cells throughout the ventricular zone, suggesting a defect in a less regionally constrained progenitor. A clearer understanding of cell lineage in the cerebral cortex could serve as a basis for interpreting genetic disorders and the genetic mechanisms of cortical development.

Experimental Procedures

Retroviral Vectors

Preparation of the AP retroviral library has been previously presented (Walsh, 1995). Size-selected genomic DNA fragments (<450 bp) from Arabidopsis thaliana were inserted into the XhoI site of the DAP plasmid (Fields-Berry et al., 1992). Bacteria from 3400 colonies were pooled, and plasmid DNA was isolated using standard techniques. Purified plasmid DNA was transfected into the CRE packaging cell line to form a transient retroviral supernatant (Cepko, 1992). Transient supernatant from ~20,000 transfected cells was then used to infect ψ2 cells (Cepko, 1992), and the resulting ~20,000 packaging colonies were selected by growth in G418-containing medium. Producer cells were grown to confluence, and retroviral supernatant was isolated, concentrated by overnight centrifugation, and stored at −80°C.

Animal Surgery

Timed-pregnant Long–Evan's (hooded) rats were purchased from Charles River's laboratories. Pregnancies were timed from the day of vaginal plug (E0). Birth usually occurred late on E21. Surgical procedures and injection of the retroviral supernatant into the lateral ventricles of fetal rat brains are described in detail elsewhere (Walsh and Cepko, 1992; Cepko et al., 1993).

Histology and Analysis of Clones

Animals were sacrificed at P15 by an overdose of Nembutal and perfused with 2%–4% paraformaldehyde in 0.1 M PIPES buffer with 2 mM $MgCl_2$, 1.25 mM EGTA. The brains were removed, submerged in fixative overnight at 4°C, and transferred to 30% sucrose in PBS at 4°C until they sank. Brains were sectioned using a Bright cryostat at 100 μm thickness. The sections were mounted onto gel-coated glass slides and processed for AP activity (Cepko et al., 1993). Labeled cells were detected by microscopic examination of tissue sections. Cell morphologies and positioning within the cortex were recorded by photography and camera lucida drawings.

Tissue Analysis with PCR

Tissue analysis was performed by preparing DNA samples from labeled cells and the surrounding unlabeled cells for amplification by PCR, as has been presented elsewhere (Walsh and Cepko, 1992, 1993). We removed the coverslips of histological slides by soaking them in a 50 ml centrifuge tube filled with sterile water. Small fragments of tissue (approximately 100 × 200 × 200 μm) containing the nucleus of each labeled cell were dissected using a fresh razor blade edge for each cell and digested with proteinase K in 1 × PCR buffer at 65°C for at least 4 hr. Each well was covered with 30 μl of mineral oil to prevent evaporation. The microtiter plate was then heated for 4–24 hr at 65°C. Once the tissue was digested, the samples were heated to 85°C to inactivate proteinase K and then heated to 95°C for 5 min to denature the genomic DNA. A nested PCR protocol was employed to increase the sensitivity and specificity of amplification and is described elsewhere (Walsh and Cepko, 1992; Walsh, 1995). At least 10% of all PCR reactions were negative controls. Any experiments that showed false PCR positives were discarded.

Analysis of PCR Products

The PCR products from the second PCR reaction were separated on 3%/1% NuSieve/Seakem agarose gels to determine tag sizes. Each tag was then digested with CfoI, RsaI, AluI, MseI, and MspI. Finally, we ran samples of similar initial size side by side on agarose gels to allow direct comparison of restriction fragment sizes.

Acknowledgments

All correspondence should be directed to C. W. The authors thank C. L. Cepko for her help and support. Research support came from National

Institutes of Health grants GM14862 (to C. R.), KO8 NS01520, and R01 NS33769 (to C. W.), from the Klingenstein Foundation Fund, and from the Rita Allen Foundation. We also thank Benxiu Ji and Wenjiang Yu for technical assistance, A. Peters for comments on neuronal cell morphology, and L. Villa-Komaroff and C. Weitz for helpful suggestions on the manuscript. We are deeply indebted to Dr. T. Blackwell for help with statistical analysis.

The costs of publication of this article were defrayed in part by the payment of page charges. This article must therefore be hereby marked *"advertisement"* in accordance with 18 USC Section 1734 solely to indicate this fact.

Received April 14, 1995; revised June 7, 1995.

References

Allendoerfer, K. L., and Shatz, C. J. (1994). The subplate, a transient neocortical structure: its role in development of connections between thalamus and cortex. Annu. Rev. Neurosci. *17*, 185–218.

Barbe, M. F., and Levitt, P. (1991). The early commitment of fetal neurons to the limbic cortex. J. Neurosci. *11*, 519–533.

Bayer, S. A., and Altman, J. (1991). Neocortical Development (New York: Raven Press).

Beaulieu, C., and Colonnier, M. (1989). Number of neurons in individual laminae of areas 3B, 4γ, and 6α of the cat cerebral cortex: a comparison with major visual areas. J. Comp. Neurol. *279*, 228–234.

Campos-Ortega, J. A. (1993). Early neurogenesis in *Drosophila melanogaster*. In The Development of *Drosophila melanogaster*, M. Bate and A. Martinez-Arias, eds. (Cold Spring Harbor, New York: Cold Spring Harbor Press), pp. 1091–1129.

Cepko, C. L. (1992). Retroviral vectors. In Current Protocols in Molecular Biology, Vol. 1, F. M. Ausubel, R. Brent, R. E. Kingston, D. D. Moore, J. G. Seidman, J. A. Smith, and K. Struhl, eds. (New York: Wiley).

Cepko, C. L., Ryder, E. F., Austin, C. P., Walsh, C., and Fekete, D. M. (1993). Lineage analysis using retroviral vectors. In Methods in Enzymology Guide to Techniques in Mouse Development, P. M. Wassarman and M. L. DePamphilis, eds. (San Diego, California: Academic Press), pp. 933–960.

Cohen-Tannoudji, M., Babinet, C., and Wassef, M. (1995). Early determination of a mouse somatosensory cortex marker. Nature *368*, 460–463.

Dallal, G. E., and Wilkinson, L. (1986). An analytic approximation to the distribution of Lilliefor's test statistic for normality. Am. Stat. *40*, 294–296.

Davis, A., and Temple, S. (1994). A self-renewing multipotential stem cell in embryonic rat cerebral cortex. Nature *372*, 263–266.

Fairen, A., DeFelipe, J., and Regidor, J. (1984). Nonpyramidal neurons: general account. In Cerebral Cortex, Vol. 1, Cellular Components of the Cerebral Cortex, E. G. Jones and A. Peters, eds. (New York: Plenum Press), pp. 201–249.

Feldman, M. L. (1984). Morphology of the neocortical pyramidal neuron. In Cerebral Cortex, Vol. 1, Cellular Components of the Cerebral Cortex, E. G. Jones and A. Peters, eds. (New York: Plenum Press), pp. 123–200.

Ferri, T., and Levitt, P. (1995). Regulation of regional differences in the differentiation of cerebral cortical neurons by EGF family-matrix interactions. Development *121*, 1151–1160.

Fields-Berry, S. C., Halliday, A. L., and Cepko, C. L. (1992). A recombinant retrovirus encoding alkaline phosphatase confirms clonal boundary assignments in lineage analysis of murine retina. Proc. Natl. Acad. Sci. USA *89*, 693–697.

Fishell, G., Mason, C. A., and Hatten, M. E. (1993). Dispersion of neural progenitors within the germinal zones of the forebrain. Nature *362*, 636–638.

Goldman, J. E., and Vaysse, P. J. J. (1991). Tracing glial cell lineages in the mammalian forebrain. Glia *4*, 149–156.

Gomez, M. (1988). Tuberous Sclerosis (New York: Raven Press).

Goodman, C. S., and Doe, C. Q. (1993). Embyronic development of the *Drosophila* central nervous system. In The Development of *Drosophila melanogaster*, M. Bate and A. Martinez-Arias, eds. (Cold Spring Harbor, New York: Cold Spring Harbor Press), pp. 1131–1206.

Gray, G. E., and Sanes, J. R. (1991). Migratory paths and phenotypic choices of clonally related cells in the avian optic tectum. Neuron *6*, 211–225.

Grove, E. A., Williams, B. P., Li, D.-Q., Hajihosseini, M., Friedrich, A., and Price, J. (1993). Multiple restricted lineages in the embryonic rat cerebral cortex. Development *117*, 553–561.

Holt, C. E., Bertsch, T. W., Ellis, H. M., and Harris, W. A. (1988). Cellular determination in the Xenopus retina is independent of lineage and birth date. Neuron *1*, 15–26.

Huttenlocher, P. R., Taravath, S., and Mojtahedi, S. (1994). Periventricular heterotopias and epilepsy. Neurology *44*, 51–55.

Luskin, M. B., Pearlman, A. L., and Sanes, J. R. (1988). Cell lineage in mouse cerebral cortex studied in vivo and in vitro with a retroviral vector. Neuron *1*, 635–647.

Luskin, M. B., Parnavelas, J. G., and Barfield, J. A. (1993). Neurons, astrocytes, and oligodendrocytes of the rat cerebral cortex originate from separate progenitor cells: an ultrastructural analysis of clonally related cells. J. Neurosci. *13*, 1730–1750.

McConnell, S. K., and Kaznowski, C. E. (1991). Cell cycle dependence of laminar determination in developing neocortex. Science *254*, 282–285.

Miller, M. W. (1986). The migration and neurochemical differentiation of γ-aminobutyric acid (GABA)-immunoreactive neurons in rat visual cortex as demonstrated by a combined immunocytochemical-autoradiographic technique. Dev. Brain Res. *28*, 41–46.

Mione, M. C., Danevic, C., Boardman, P., Harris, B., and Parnavelas, J. (1994). Lineage analysis reveals neurotransmitter (GABA or glutamate) but not calcium-binding protein homogeneity in clonally related neurons. J. Neurosci. *14*, 107–123.

O'Rourke, N. A., Dailey, M. E., Smith, S. J., and McConnell, S. K. (1992). Diverse migratory pathways in the developing cerebral cortex. Science *258*, 299–302.

Parnavelas, J. G., Barfield, J. A., Franke, E., and Luskin, M. B. (1991). Separate progenitor cells give rise to pyramidal and nonpyramidal neurons in the rat telencephalon. Cereb. Cortex *1*, 1047–3211.

Peters, A., and Jones, E. G. (1984). Classification of cortical neurons. In Cerebral Cortex, Vol. 1, Cellular Components of the Cerebral Cortex, E. G. Jones and A. Peters, eds. (New York: Plenum Press), pp. 107–122.

Peters, A., and Kara, D. (1985). The neuronal composition of area 17 of the rat visual cortex. I. The pyramidal cells. J. Comp. Neurol. *234*, 218–241.

Price, J., and Thurlow, L. (1988). Cell lineage in the rat cerebral cortex: a study using retroviral-mediated gene transfer. Development *104*, 473–482.

Rakic, P. (1972). Mode of migration to the superficial layers of fetal monkey neocortex. J. Comp. Neurol. *145*, 61–84.

Reynolds, B. A., and Weiss, S. (1992). Generation of neurons and astrocytes from isolated cells of the adult mammalian central nervous system. Science *255*, 1707–1710.

Simoens, C. R., Gielen, J., Van Montagu, M., and Inze, D. (1988). Characterization of highly repetitive sequences of *Arabidopsis thaliana*. Nucl. Acids Res. *16*, 6753–6766.

Stemple, D. L., and Anderson, D. J. (1992). Isolation of a stem cell for neurons and glia from the mammalian neural crest. Cell *71*, 973–985.

Temple, S. (1989). Division and differentiation of isolated CNS blast cells in microculture. Nature *340*, 471–473.

Turner, D. L., Snyder, E. Y., and Cepko, C. L. (1990). Lineage-independent determination of cell type in the embryonic mouse retina. Neuron *4*, 833–845.

Waechter, R., and Jaensch, B. (1972). Generation times of the matrix cells during embryonic brain development: an autoradiographic study in rats. Brain Res. *46*, 235–250.

Walsh, C. (1995). PCR-based techniques for cell lineage analysis using

retroviruses. Meth. Mol. Genet. *4*, in press.

Walsh, C., and Cepko, C. L. (1988). Clonally related neurons show several patterns of migration in cerebral cortex. Science *255*, 1342–1345.

Walsh, C., and Cepko, C. L. (1992). Widespread dispersion of neuronal clones across functional regions of the cerebral cortex. Science *241*, 434–440.

Walsh, C., and Cepko, C. L. (1993). Widespread clonal dispersion in proliferative layers of cerebral cortex. Nature *362*, 632–635.

Walsh, C., Cepko, C. L., Ryder, E. F., Church, G. M., and Tabin, C. (1992). The dispersion of neuronal clones across the cerebral cortex: response. Science *258*, 317–320.

Werner, L., Hedlich, A., and Winkelmann, E. (1985). Neurontypen im visuellen Kortex der Ratte, identifiziert in Nissl- und deimprägnierten Golgi-Präparaten. J. Hirnforsch. *26*, 173–186.